Journal of Materials Chemistry B

Accepted Manuscript

ROYAL SOCIETY OF CHEMISTRY

www.rsc.org/materialsB

Journal Name

RSCPublishing

ARTICLE

Enzyme-inorganic hybrid nanoflowers based immobilized enzyme reactor with enhanced enzymatic activity

Yuqing Yin,[a†] Yun Xiao,[a†] Guo Lin,[a] Qi Xiao,[a] Zian Lin*[a,b] and Zongwei Cai[b]

Cite this: DOI: 10.1039/x0xx00000x

Received 00th January 2012,
Accepted 00th January 2012

DOI: 10.1039/x0xx00000x

www.rsc.org/

A facile approach for the synthesis of enzyme-inorganic hybrid nanoflowers and its application as an immobilized α-chymotrypsin (ChT) reactor (IMER) for highly efficient protein digestion was described. The hybrid nanoflowers were room-temperature synthesized in aqueous solution using calcium phosphate ($Ca_3(PO_4)_2$) as the inorganic component and ChT as the organic component. The effects of reaction parameters on the formation of the enzyme-embedded hybrid nanoflowers and its growth mechanism were investigated systematically. By monitoring the reaction of N-benzoyl-L-tyrosine ethyl ester (BTEE), the enzymatic activity of the immobilized ChT was calculated and the results showed 266% enhancement in enzymatic activity. The performance of such a nanoreactor was further demonstrated by digesting bovine serum albumin (BSA) and human serum albumin (HSA), with a stringent threshold for unambiguous identification of these digests, the yielding sequence coverage for nanoflower-based digestion were 48% and 34%, higher than those obtained with the free enzyme. Whereas the digestion time of BSA and HSA in the former case was less than 2 min, about 1/360 of that performed in the latter case (12 h). Furthermore, the residual activity of the nanoflowers decreased slightly even after eight repeated use, demonstrating promising stability. In addition, the hybrid nanoflower-based IMER was applicable to the digestion of complex human sample, showing great promise for proteome analysis.

Introduction

Proteolytic digestion followed by mass spectrometry (MS) analysis of the resulting fragments is the most common method to indentify proteins and investigate post-translational modifications.[1] Typically, digestion occurs upon mixing proteases such as trypsin, lys-C, or α-chymotrypsin (ChT) with substrate proteins in buffer solutions, but it often suffers from several drawbacks such as long digestion time (up to 24 h), enzyme autodigestion, low stability of the enzyme to environmental changes (heat, organic solvents, or pH), and difficult recovery of enzymes.[2,3] These problems can be overcome to some extent by enzyme immobilization on solid supports (defined as immobilized enzyme reactors, IMERs), which provide predominant advantages including high enzyme-to-substrate ratio, great enzyme stability and reusability, good digestion efficiency, as well as short digestion time.[4] In the past decades, considerable efforts have been made for developing various solid supports to overcome this problem, which included pore glassbeads,[5] nanoparticles,[6-8] membranes,[9] glass,[10] and polymer-/silica-based monolithic materials[11-13] that were covalently bonded or physically adsorbed with protease. Although these IMERs have achieved some success, probing new supporting materialsas efficient IMERs is becoming an urgent topic for extending the application in proteomics.

Nanobiocatalysis, using nanostructured materials for enzyme immobilization, has gathered growing attention due to its recent successes in stabilizing the enzyme activity.[14] Various nanobiocatalytic supports including nanoporous media, nanofibers, carbon nanotubes, and nanoparticles have been found to be efficient in manipulating the nanoscale environment of the enzyme and thus promising exciting advances in many areas of enzyme technology.[15,16] Flower-like nanomaterials (nanoflowers), possessing of large surface-to-volume ratio compared with that of bulk materials, are not currently reported so frequently as nanotubes or nanobeads due to their extremely harsh synthetic conditions. Up to now, although various approaches have been developed to synthesize nanoflowers, more attempts are focused on oxidation of elemental metals, reduction of metal salts, thermal decomposition of relatively unstable compounds, and electrochemical routes.[17] Among them, special precautions should be taken to avoid uncontrolled growth or morphological deformations since they tend to be employed with harsh conditions (high temperature and pressure and the use of toxic organic solvents). As a result, a facile, versatile and cost effective synthetic method for obtaining the

controlled and well-defined hierarchical nanoflowers is highly desirable. Recently, an encouraging breakthrough in synthesis of immobilized enzymes with greatly enhanced activities was achieved by Zare's group,[18] who firstly reported the novel synthesis of hybrid nanoflowers comprising of $Cu_3(PO_4)_2$ and proteins via a coprecipitation method. On the basis of the principle, our group[19] also prepared $Cu_3(PO_4)_2$-trypsin hybrid nanoflowers and then applied it as a novel IMER platform for highly efficient protein digestion for the first time. Lately, Wang *et al.*[20] developed a new method for synthesis of $CaHPO_4$-α-amylase hybrid nanoflowers based on allosteric effect, and explained the mechanism of the increase in catalytic activity when certain enzymes are immobilized in specific nanomaterials. Despite this attractive feature of the enzyme-$CaHPO_4$ hybrid nanoflowers, the advantages of the hybrid nanoflowers have not been fully demonstrated yet. Further development is necessary to explore new applications of this type of hybrid nanoflowers.

Herein, we report an approach for the preparation of enzyme-inorganic hybrid nanoflowers using calcium phosphate ($Ca_3(PO_4)_2$) as the inorganic component and α-chymotrypsin (ChT) as the organic component. The as-prepared hybrid nanoflowers have an interesting structure containing of micrometre-sized particles and nanoscale flower-like petals. Significantly, the $Ca_3(PO_4)_2$-ChT hybrid nanoflowers, applied as a novel IMER, exhibit higher proteolytic performance toward standard protein and complex protein sample than the free enzyme. In addition, the hybrid nanoflowers have good regenerability and stability, enabling repeated usage for protein digestion without significant loss of enzymatic activity, showing their potential application in proteome analysis.

Experimental

Reagents and Materials

All other chemicals were of analytical grade or better. Calcium chloride anhydrous ($CaCl_2$) was purchased from Sinopharm Chemical Reagent, Co., Ltd (Shanghai, China). Iodoacetamide (IAA), 1,4-dithiothreitol (DTT), formic acid (FA), acetonitrile (ACN, HPLC grade), bovine serum albumin (BSA), human serum albumin (HSA) and ChT were obtained from Sigma (St. Louis, MO). N-phenyl ethyl formyl-L-tyrosine (BTEE，Mw 313.4, Purity> 98%) was the product of Shanghai Dong Feng Biochemical Technology Company (Shanghai, China). The deionized water used in all experiments was purified with a Milli-Q system from Millipore (Milford, MA). Healthy human serum sample was kindly gifted from Fujian Province Official Hospital (Fuzhou, China).

Synthesis of enzyme-inorganic hybrid nanoflowers

$Ca_3(PO_4)_2$-ChT hybrid nanoflowers was synthesized according to the previous work [20] with some modifications. Briefly, 90 μL of aqueous $CaCl_2$solution (200 mM) was added into 4.5 mL of phosphate buffered saline (PBS) solution (4mM, pH 7.4) containing different concentrations of ChT. The reaction was then allowed to proceed at room temperature for 12 h. The products were centrifuged at 12,000 rpm for 10 min and washed with water three times.

Characterizations

Scanning electron micrographs (SEM) of the prepared hybrid nanoflowers were carried out on a XL-30E scanning electron microscope (Philips, Netherlands). Fourier transform infrared (FT-IR) spectra of the nanoflowers were conducted with a FT-IR spectrophotometer (Nicolet 6700, Waltham, MA, USA). The crystal structures of the nanoflowers were determined by X-ray powder diffraction (XRD) (D/Max-2500 diffractometer, Shimadzu, Japan). The energy-dispersive X-ray spectroscopy (EDX) analysis was also done with a JEOL2010 transmission electron microscope (TEM) (JEOL, USA).Surface area and pore size analysis of the nanoflowers were performed by Brunauer-Emmett-Teller (BET) and Barrett-Joyner-Halenda (BJH) methods using physisorption analyzer (Micromeritics ASAP2020 porosimeter, USA). The data of adsorption were obtained by using UV/Vis spectrophotometer (Shimadzu UV2550, Japan). The encapsulation yield of ChT was obtained by determining the supernatant at 280 nm using the UV/Vis spectrophotometer and weight percentage of ChT in the nanoflowers was determined by the gravimetric method. Analysis of digested peptides was performed with LC-ESI-Q-TOF/MS (Agilent, Palo Alto, CA, U.S.A.).

Measurement of the ChT activity

The catalytic activity of ChT was determined using BTEE as the substrate. For this purpose, some modifications were made to determine the activity of immobilized ChT following the method developed by Tian[21] and Brown.[22] Briefly, 0.2 mg of the ChT-immobilized nanoflowers was dissolved in 40 μL, 10mM Tris-HCl buffer (pH7.8). The blank solution, which contained 280 μL, 0.5 mM BTEE in 40μL, 10mM Tris-HCl buffer (pH 7.8), was used to calibrate the UV/Vis spectrophotometer at 256 nm; then a total of 280 μL, 0.5 mM BTEE was hydrolyzed with nanoflowers at 25 ºC and the increase in absorbance at 256 nm was measured every 30 s for 20 min. Finally, the kinetics curves with regards to the enzymatic reaction were drawn. The bioactivity was calculated in BTEE-units/mg ChT, and 1 BTEE-unit is equal to an increase in absorbance of 0.001/min at 256 nm under specific conditions. The activity was calculated with following equations:

$$\text{The activity (BTEE unit/mL)} = (\Delta A256/\text{min}) / (0.001 \times V(\text{ChT})) \quad (1)$$

$$\text{The activity (BTEE unit/mg)} = \text{The activity (BTEE unit/mL)} / (\text{concentration of ChT(mg/mL)} \times V(\text{ChT})) \quad (2)$$

In the case of free ChT, the activity measurement was done following the procedures and the conditions similar to those for immobilized ChT.

Digestion of proteins and human serum using hybrid nanoflowers

1.0 mg BSA (or HSA) in 1.0 mL of 50 mM NH_4HCO_3 buffer solution (pH 8.0) (or 10 μL human serum in 590 μL of 50 mM NH_4HCO_3 buffer solution (pH 8.0), which corresponds to 600 μg total proteins by Brandford protein assay (Bio-Rad, Catalog. No. P0006) using BSA a standard) was denatured in a 95 ºC water bath for 5 min and then reduced in 15% (v/v) ACN and 5 mM DTT for 1h at 56 ºC. When cooled to room temperature, cysteines were alkylated in the dark in 10 mM IAA for 1h at room temperature. Subsequently, 0.10 mg dried nanoflowers was transferred to 300 μL of the above denatured protein solution (substrate-to-enzyme ratio of 30:1) in a 1.5 mL Eppendorf tube at 37 ºC for 5min. The supernatant was collected and directly analyzed by LC-ESI-Q-TOF/MS.

For comparison, the digestion of protein and human serum using free ChT was also performed according to the conventional procedures. After alkylation, digestion was performed by adding free ChT into the pretreated protein sample with a substrate-to-enzyme ratio of 30:1(m/m). Then the solution was incubated at 37 ºC for 12h. After the digestion, 1% (v/v) formic acid (FA) was added to stop the reaction.

MS analysis and database searching

The chymotryptic peptides were separated by reversed-phase HPLC using an Agilent 1260 HPLC. An Agilent C18 column (50 mm × 3 mm i.d.) packed with a 2.7 μm diameter particles, 120 Å pore size C18 resin was used for the separations. The solvents were as follow: (A) 0.1 % FA in water, and (B) 0.1 % FA in ACN. The column was equilibrated at 3 % solvent B. Three minute after sample injection the concentration of buffer B was increased from 3 to 40% B within 20 min followed by a linear gradient of 40% to 80% B over 3 min. A flush step was performed with 80% B for 3 min and the column was equilibrated with 3 % B for 4 min. The column temperature was maintained at 40 °C.

MS detection was performed on an Agilent 6520 Q-TOF mass spectrometer with a dual ESI source and an Agilent G1607A coaxial sprayer (all from Agilent). All analyses were performed in a positive ion mode. Nitrogen was used as drying gas at a temperature of 350 °C and a flow-rate of 10 L min^{-1}. The voltage set for the MS capillary was 4 kV and the fragmentor was set to 175 V. Scanning mass range was from m/z 100 to 3000 at an acquisition rate of 3 spectra s^{-1} in the auto MS/MS mode. For MS^2 experiments, the collision energy was set to according to formula, in which the top three highest intensity peaks in each MS were chosen for collision-induced dissociation. Isolation width for MS^2 was ± 4 amu.

All the LC-MS/MS data were searched with Spectrum Mill versionA.03.03 against a database (target database of IPI bovine v3.80, IPI plants v3.80, and IPI human.v3.80). Chymotrypsin restriction was set with two missed cleavages. Cyscarboxymethylation was set as the static modification. Oxidized methionine and proglutamic acid were set as the variable modifications. The mass tolerances were 100 ppm for parent ions and 200 amu for fragment ions.

Stability and reusability

The stability of the immobilized ChT was assessed after storing at -20°C for 30 days. In order to avoid the loss of nanoflowers during washing process, a home-made digestion device was designed for cycle experiment. In brief, 0.10 mg nanoflowers was packed into a pipette tip that was beforehand filled with a sieve, and then 300 μL of the above denatured protein solution was pipetted into the tip. After incubating at 37°C for 2 min, the solution was pushed and collected for MS analysis. Then the tip was washed two times with 10 μL of 50 mM NH_4HCO_3 buffer solution (pH 8.0), and then resuspended in the same buffer to start a new run. The bioactivity to biomacromolecule were expressed in the way that the percentage of residual activity to the initial one.

Results and Discussion

Synthesis and characterization of enzyme-inorganic hybrid nanoflowers

As illustrated in Fig.1(a), enzyme-inorganic hybrid nanoflowers were synthesized in one pot by adding 90μL of aqueous $CaCl_2$ solution to 4.5 mL of PBS solution containing ChT, at pH 7.4 and room temperature. After incubation for 12 h, a white precipitate with porous, flower-like structures was obtained. Fig.1(b-d) showed the SEM images of the ChT-inorganic nanoflowers. In the low-resolution SEM images, most of the hybrid nanoflowers were uniform architectures (Fig.1(b-c)). The high-resolution SEM image (Fig.1(d)) showed that the hybrid nanoflowers have a hierarchical dahlia-like flower morphology, which was assembled from hundreds of nanoplates (the lower right of Fig.1 (d)). For example, the average diameter of a single nanoflower was ~ 20 μm was obtained while using 0.1 $mgmL^{-1}$ ChT.

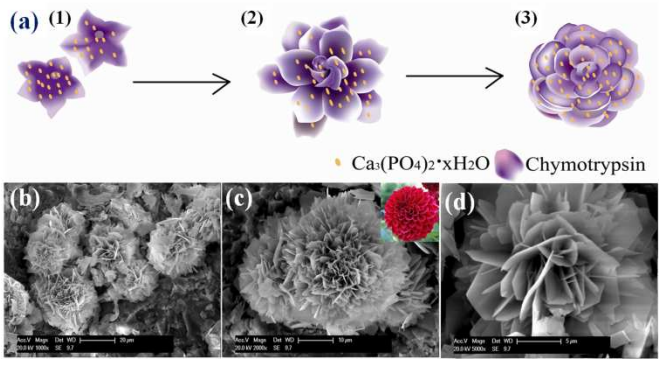

Fig.1 Hybrid nanoflowers made fromChT and $Cu_3(PO_4)^2$. (a) Schematic representation of the synthesis of hybrid nanoflowers; (b-d) SEM images of the hybrid nanoflowers obtained from an aqueous solution of 0.1 $mgmL^{-1}$ ChT, 200 mM Ca^{2+}, 4 mM PBS at pH 7.4.

The effect of ChT concentration on the formation of hybrid nanoflowers was investigated (Fig.2). In the absence of ChT, large crystals, but no nanoflowers were formed (Fig.2a). However, the flower-like nanostructures emerged when ChT

was added. It was observed that some small buds appeared (Fig. 2b) when using 0.05 mg mL^{-1} ChT. Gradually increasing the concentration of ChT from 0.05 to 0.1 mg mL^{-1}, the morphology of the nanoflowers changed significantly, and mimicking the growth process of flowers in nature was observed from small bud to bloom (Fig. 2c). Accordingly, the average diameters of these nanoflowers increased from ~2 μm to ~20 μm. Finally, Fig.2d clearly demonstrated scattered petals which were formed in the presence of a relatively high concentration of ChT (0.5 mg mL^{-1}).

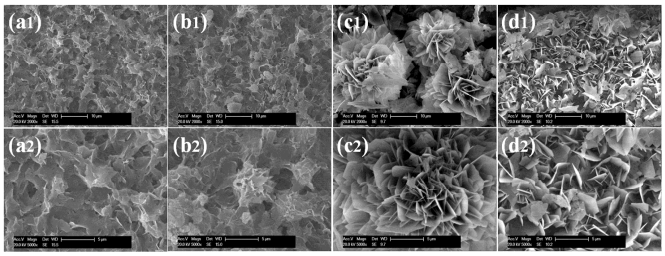

Fig.2 Effect of different ChT concentrations on the morphologies of nanoflowers. (a1-2) 0.0 mg mL^{-1}; (b1-2) 0.05 mg mL^{-1}; (c1-2) 0.1 mg mL^{-1}; (d1-2) 0.5 mg mL^{-1}; Other conditions: 200 mM Ca^{2+}, 4 mM PBS at pH 7.4, and reaction for 12 h at 25 ℃.

FT-IR spectroscopy provides a direct proof for the synthetic process of the hybrid nanoflowers (Fig.3). The strong IR band (spectrum a and c) at 1031 cm^{-1} was characteristic of the P-O vibrations and stretches, while the bands at 566 cm^{-1} and 603 cm^{-1}may be attributed to the bending vibrations of bridging phosphorous such as O=P-O, indicating the existence of phosphate groups. Compared to spectrum a and b, the typical bands of ChT at 1400~1644 cm^{-1} for $–NH_2$, and 2800-3000 cm^{-1} for $–CH_2$ and $–CH_3$ were observed in spectrum c. Moreover, the hybrid nanoflowers in spectrum c did not show new adsorption peaks and significant peak shift, indicating ChT was immobilized via self-assembly, instead of covalent bonding. EDS experiment (Fig. S1 in the ESI†) revealed that the formed precipitate was constituted by an aggregate with amorphous $Ca_3(PO_4)_2$•nH_2O crystals that disperse into an organic ChT component. XRD analysis (Fig. S2 in the ESI†) confirmed the positions and relative intensities of all diffraction peaks of $Ca_3(PO_4)_2$•nH_2O matched well with those obtained from the JCPDS card (00-018-0303). The sharp, strong peaks confirmed the hybrid nanoflowers were well crystallized and had high crystallinity after incorporating ChT.

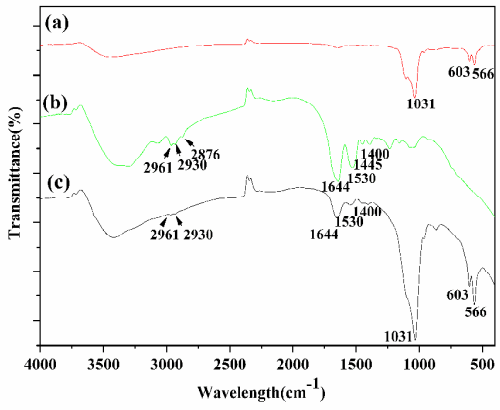

Fig.3 FT-IR spectra of (a) $Ca_3(PO_4)_2.nH_2O$; (b) ChT; (c) the ChT-inorganic hybrid nanoflowers.

In addition, the surface area, pore volume and average pore diameter were measured using the BET method (Fig.S3 in the ESI†) and their corresponding values were 91.81 $m^2\ g^{-1}$, 0.271 $cm^3\ g^{-1}$ and 118.23 nm, indicating the presence of the porous structure and high surface-to-volume ratio in the hybrid nanoflowers.

Binding amount of ChT in hybrid nanoflowers

The actual encapsulation efficiency (defined as the ratio of the amount of immobilized ChT to the total amount of ChT employed) and weight percentages of ChT in the nanoflowers were further determined by colorimetric and gravimetric methods, respectively. The results (Table S1 in the ESI†) demonstrated the weight percentage of ChT embedded in the nanoflowers gradually increased from 8.029% to 26.75% as the ChT concentration increased from 0.05 to 0.5 mg mL^{-1}, and then down to 8.03% with continuously increasing ChT concentration from 0.5 to 1.0 mg mL^{-1}. Obviously, excessive addition of ChT to a constant inorganic component may induce the dramatic decrease of encapsulation efficiency. However, a relatively high encapsulation yield of 20.31% was obtained as the ChT concentration was 0.1 mg mL^{-1}, and a proper weight percentage of 10.70% was achieved in comparison to those obtained in the low concentrations of ChT. Based on the above results, the hybrid nanoflowers with 0.1mg mL^{-1} ChT was chosen as the best for further evaluation and applications considering its good morphology and high weight percentage.

Catalytic activity of hybrid nanoflowers

The catalytic activity of the hybrid nanoflowers was evaluated using BTEE as the substrate according to the method described previously.[21,22] The absorbance of different systems (nanoflowers and free ChT) was demonstrated in Fig. 4(a). The plot lies on the premise of setting initial concentrations of BTEE to 0.5 mM. Upon the addition of ChT, absorbance at 256 nm increased slowly and reached the platform over 15 min. However, in ChT-embedded nanoflower system (the concentrations of ChT put in were all 1.2 mg mL^{-1}), same absorbance could be obtained within 5 min, indicating the high catalytic efficiency of the nanoflowers. The pseudofirst-order kinetics with respect to BTEE could be applied to our experimental system. As shown in the insert part of Fig. 4(a), the approximately linear shape of the plot $-\ln I_{sub}$ (I_{sub} is the value obtained by subtracting the real-time absorbance from the saturated one) *vs.* time supports the pseudofirst-order assumption. Based on it, the average reaction rate constants (k) were calculated to 1.36 min^{-1} and 0.167 min^{-1} when nanoflowers and free ChT were used, respectively. In addition, the enzymatic activity of the ChT-embedded nanoflowers was determined to be 3410 U mg^{-1}, approximately 266% higher than free ChT in solution (1123 U mg^{-1}). Although the increased extent of enzymatic activity is not high compared to the previous works,[18,23] where 506~650% enhancement in enzymatic activity was reported using horseradish peroxidise

(HRP)/or laccase-embedded hybrid nanoflowers, it is speculated that the increased extent was dependent not only on the morphology of nanoflowers, but also on the quality of enzyme used. Overall, the enhancement in the enzymatic activity of ChT-embedded nanoflowers compared to free ChT catalysis can be ascribed to (1) minimization or elimination of autolysis ofChT and (2) the possible stabilization of nanoflower-like structure of ChT with high surface area and confinement, resulting in higher accessibility of the substrate to the active sites of the enzyme.

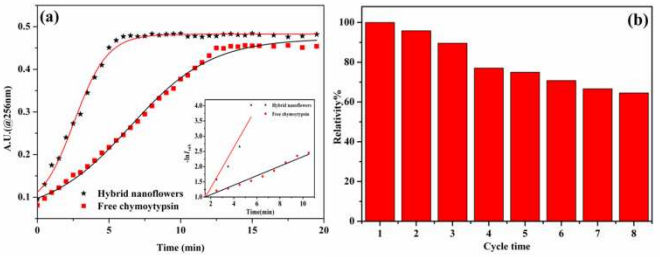

Fig. 4(a) Catalytic kinetics and reaction rate (insert part) of the esterlysis of BTEE by free ChT (■) and hybrid nanoflowers (★). (B)The stability and durability of hybrid nanoflowers after stored at -20 ℃ for 30 days.

Protein analysis

The performance of the nanoflower-based reactor was evaluated by digesting 1.0 mg mL^{-1} BSA and HSA. Table 1 listed the database searching results of BSA digested by free ChT and the ChT-embedded nanoflower reactors. It was observed from Table 1 (and Table S2 in the ESI†) that the total sequence coverage and the number of matched peptides for BSA obtained with the nanoflower reactor was found to be 48% and 39 matched peptides within 2 min, comparable with those obtained with free ChT, where the sequence coverage of 41% and 36 matched peptides were detected with 12h, indicating that good enzymatic efficiency of nanoflowers. Compared with other immobilized ChT reactors[24,25], the nanoflower-based IMER could offer higher enzymatic activity and faster digestion, which confirmed the superiority of the nanoflower-based reactor. It was worth to note that high level of sequence coverage and matched peptides can be achieved, even after being stored at -20 ºC for 30 days. The result indicated the excellent stability of the nanoflower-based reactor. Similar results (Table 1 and S3 in the ESI†) were obtained using HSA as target protein, where 33 matched peptides with the sequence coverage of 34% could be obtained within 2 min, higher than that performed in solution digestion (27 matched peptides with the sequence coverage of 32%).

Table1. Comparison of the efficiency of hybrid nanoflower reactors and solution digestion method on protein proteolysis (n=3)

Methods	BSA digestion		HSA digestion	
	Sequence coverage [%]	Peptide matches	Sequence coverage [%]	Peptide matches
Free[a]	41	36	32	27
Nanoflowers[b]	48	39	34	33
Nanoflowers[c]	43	32	----[d]	----[d]

[a]Free ChT with 12 h of digestion at 37℃.
[b]Nanoflowers within 2 min of digestion at 37℃.
[c]Nanoflowers were stored at -20℃ for 30 days.
d not done

Real sample analysis

The attractive enzymatic hydrolysis efficiency of ChT-embedded hybrid nanoflowers makes it possible to digest human serum. The results were showed (Tables S4-5 in the ESI†) that 9 proteins (n=3), including three low-abundance proteins (alpha-1B-glycoprotein, beta-2-glycoprotein, alpha-2-HS-glycoprotein) were identified within 2 min digestion by the nanoflowers, better than those obtained by free ChT digestion (12 h), where 8 proteins were discovered (n=3), but no low-abundance proteins. Therefore, the nanoflowers exhibited good proteolytic performance for the digestion of complex sample.

Stability and durability

The reusability and stability of the nanoflowers were tested by batch hydrolysis of BSA. The home made digestion device as depicted in Fig.S4 (ESI†) was used in order to avoid the loss of nanoflowers during washing process. It was observed from Fig.4(b) that the residual activity of the nanoflowers toward BSA decreased slightly as the cycle number increased, although they still showed high degree of activity recovery after eight cycles. The slight decrease in enzyme activity may be come from the loss of nanoflowers during the eluting process. Nevertheless, the nanoflowers still exhibited promising stability even after multiple cycle use. In addition, it was worth noting that no obvious deformation in the morphology was observed after eight cycles (data no shown), indicating that the nanoflowers have good mechanical stability.

Conclusions

In conclusion, we reported a facile method for the synthesis of enzyme co-embedded organic-inorganic hybrid nanoflowers by using ChT as the organic components and calcium (II) ions as the inorganic component. The synthetic method was very simple and efficient. The resultant hybrid nanoflowers have hierarchical flower-like structure with high surface area and enhanced catalytic activity. Significantly, the resulting nanoflowers could be used as an enzyme reactor for the high-efficiency digestion of proteins. The successful application in real sample analysis suggests that the hybrid nanoflowers have great potential in proteomic analysis.

Acknowledgements

This study was supported by the National Natural Science Foundation of China (21375018 and 21175025), and the Natural Science Foundation of Fujian Province (2014J01402).

a. Ministry of Education Key Laboratory of Analysis and Detection for Food Safety, College of Chemistry, Fuzhou University, Fuzhou, Fujian, 350116, China
b. Partner State Key Laboratory of Environmental and Biological Analysis, Department of Chemistry, Hong Kong Baptist University, 224 Waterloo Road, Kowloon Tong, Hong Kong, SAR, P. R. China
Fax: (+86)591-22866135
♀The first two authors contributed equally to this paper
E-mail: zianlin@fzu.edu.cn (L.A.Lin);
†Electronic supplementary information (ESI) available: Experimental details and additional figures.

Notes and references

1. X. Han, A. Aslanian, and J. R. Yates, *Curr. Opin. Chem. Biol.*, 2008, **12**, 483-490.
2. A. Popat, S. B. Hartono, F. Stahr, J. Liu, S. Z. Qiao and G. Q. Lu, *Nanoscale* 2011, **3**, 2801-2818.
3. R. A. Sheldon, *Adv. Synth. Catal.*, 2007, **349**, 1289-1307.
4. J. Krenkova, N. A. Lacher, and F. Svec, *Anal. Chem.*, 2009, **81**, 2004-2012.
5..E. Yilmaz, K. Can, M. Sezgin, and M. Yilmaz, *Bioresour. Technol.*, 2011, **102**, 499-506.
6. Y. Li, X. Q. Xu, B.Yan, C. H. Deng, W. J. Yu, P. G. Yang, and X. G. Zhang, *Proteomics*, 2007, **7**, 2330-2339.
7. H. L. He, X. L. Xu, H. X. Wu, Y. J. Zhai, and Y. D. Jin, *Anal. Chem*. 2013, **85**, 4546-4553
8. M. Filice, M. Marciello, M. D. P. Morales, and J. M. Palomo, *Chem. Commun.*, 2013, **49**, 6876-6878.
9. P. Jochems, Y. Satyawali, L. Diels, and W. Dejonghe, *Green Chem.*, 2011, **13**, 1609-1623.
10. E. Bonneil, M. Mercier and K. C. Waldron, *Anal. Chim. Acta* 2000, **404**, 29-45.
11. J. F. Ma, C. Y. Hou, Y. Liang, T. T. Wang, Z. Liang, and Y. H. Zhang, *Proteomics*, 2011, **11**, 991-995.
12.R. A. Sheldon, *Adv. Synth. Catal.*, 2007, **349**, 1289-1307.
13. Z. Zhou and M. Hartmann, *Chem. Soc. Rev.*, 2013, **42**, 3894-912.
14. J. Y. Sun, J. C. Ge, W. M. Liu, M. H. Lan, H. Y. Zhang, P. Y. Wang, Y. M. Wang, and Z. W. Niu, *Nanoscale*, 2014, **6**, 255-262.
15. R. X. Wang, Z. G. Tian, and L. G. Chen, *Int. J. Pharm.*, 2011, **406**, 153-162.
16. R. Prakasham, G. Devi, C. Rao, V. Sivakumar, T. Sathish, and P. Sarma, *Appl. Biochem. Biotechnol.*, 2010, **160**, 1888-1895.
17. B. T. Zhang, L. L. Lu, Q. C. Hu, F. Huang, and Z. Lin, *Biosens. Bioelectron.*, 2014, **56**, 243-249.
18. J. Ge, J. D. Lei, and R. N.Zare, *Nat. Nanotechnol.,* 2012, **7**, 428-432.
19. Z. A. Lin, Y. Xiao, L. Wang, Y. Q. Yin, J. N. Zheng, H. H. Yang, and G. N. Chen, *RSC Adv*. 2014, **4**,13888-13891.
120. L. B. Wang, Y. C. Wang, R. He, A. Zhuang, X. P. Wang, J. Zeng, and J. G. Hou, *J. Am. Chem.Soc.*, 2013, **135**, 1272-1275.
21. W. X. Tian, and C. L. Tsou, *Biochemistry*, 1982, **21**, 1028-1032.
22. J. J.Brown, and T. W.Perry, *J. Anim. Sci.*, 1981, **52**, 359-362.
23. Z.A. Lin, Y. Xiao, Y.Q. Yin, W.L. Hu, W. Liu, and H.H. Yang, *ACS. Appl. Mater. Interfaces*. 2014, **6**, 10775-10782.
24. S. Wang, T. Liu, L. Y. Zhang, G. Chen, and P. G. Yang, *J. proteomics*, 2009, **72**, 640-647.
25. S. Wang, T. Liu, L. Y. Zhang, G. Chen, and P. G. Yang, *J. Proteome Res.*, 2008, **7**, 5049-5054.

Table of contents entry

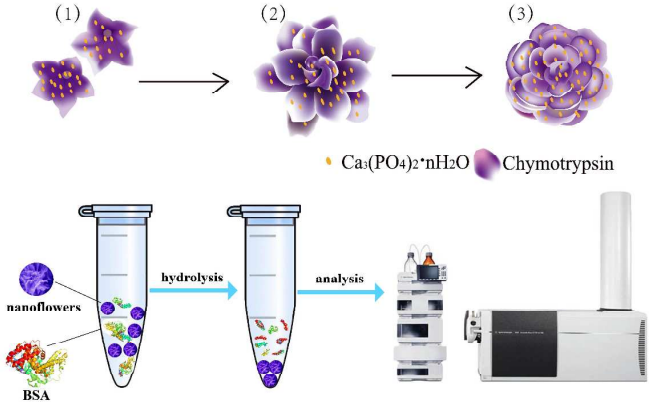

$Ca_3(PO_4)_2$-ChT hybrid nanoflowers were synthesized by a facile approach. The nanoflowers exhibited an enhanced enzymatic activity and can be used as an immobilized enzyme reactor (IMER) for highly efficient protein digestion.